

Developing V_{S30} Site-Condition Maps by Combining Observations with Geologic and Topographic Constraints



E. M. Thompson

Tufts University, Medford MA USA

D. J. Wald

U.S. Geological Survey, Golden CO USA

SUMMARY

Despite obvious limitations as a proxy for site amplification, the use of time-averaged shear-wave velocity over the top 30 m (V_{S30}) remains widely practiced, most notably through its use as an explanatory variable in ground motion prediction equations (and thus hazard maps and ShakeMaps, among other applications). As such, we are developing an improved strategy for producing V_{S30} maps given the common observational constraints. Using the abundant V_{S30} measurements in Taiwan, we compare alternative mapping methods that combine topographic slope, surface geology, and spatial correlation structure. The different V_{S30} mapping algorithms are distinguished by the way that slope and geology are combined to define a spatial model of V_{S30} . We consider the globally applicable slope-only model as a baseline to which we compare two methods of combining both slope and geology. For both hybrid approaches, we model spatial correlation structure of the residuals using the kriging-with-a-trend technique, which brings the map into closer agreement with the observations. Cross validation indicates that we can reduce the uncertainty of the V_{S30} map by up to 16% relative to the slope-only approach.

Keywords: Site response, hybrid, geology, slope, Taiwan, geostatistics

1. INTRODUCTION

For seismic hazard assessments, the importance of the near-surface shear-wave velocity (V_S), specifically the time-averaged V_S to 30 m depth (V_{S30}), arises primarily from its use in international building codes (International Code Council, 2006) and its use as the explanatory variable for site response in ground motion prediction equations (GMPEs; e.g., Abrahamson et al., 2008). GMPEs such as these are a fundamental component of the National Seismic Hazards Maps (Petersen et al., 2008) and rapid response maps (U.S. Geological Survey's ShakeMap and PAGER systems).

Efforts to map site response date back to Tinsley and Fumal (1985). They presented an index of site amplification that is primarily based on soil type, age, and the average V_S range of the geologic unit. Other efforts have built upon this method, and generally focus on correlations of V_{S30} with some other variable that is easily measured at the scale and resolution of interest. This includes correlations with surficial geology (Romero and Rix, 2001; Wills and Clahan, 2006), topographic slope (Wald and Allen, 2007; Allen and Wald, 2009), and geomorphologic terrain mapping from satellite imagery (Yong et al., 2008; Yong et al., 2012). Other efforts have focused on achieving more accurate results for smaller regions (Holzer et al., 2005; Thompson et al., 2010; Thompson et al., 2011), which are often referred to as “microzonation” studies. Each of these efforts represents a different compromise between precision and the spatial extent of the mapped region. The spatial coverage and data density required by these different approaches varies by many orders of magnitudes, and thus a hierarchical approach is needed to achieve the best possible estimate for a given location.

Wald et al. (2011) proposed a V_{S30} mapping strategy that is hierarchical, combining different constraints on V_{S30} such as geology and topographic slope. Magistrale et al. (2012) presented a map of the US that uses a similar approach by defining a different slope- V_{S30} relationship for young lacustrine regions. Thompson et al. (2010) advocated for a geostatistical method of kriging-with-a-trend where the trend is defined as the mean V_{S30} for each geologic unit. This was a hierarchical model in the sense

that for locations in the vicinity of measurements the map is controlled by the measured values, but the map reverts to a geology-based trend at locations distant from the observations. Thompson et al. (2011) expanded on this method to combine multiple site response estimates (including geology and topographic slope) with a weighted mean, where the weights are defined as the inverse of the prediction variance.

In this paper we use the kriging-with-a-trend V_{S30} mapping approach and focus on different ways to define the trend. We use the abundant V_{S30} measurements in Taiwan to assess the accuracy of V_{S30} maps where the trend is a function of geology, topographic slope, or both. We consider two different methods for combining slope and geology. We compare these alternative V_{S30} maps in terms of the standard deviation of the residuals.

2. DATA

The National Center for Research on Earthquake Engineering (NCREE) has built a database of 447 V_{S30} measurements in Taiwan (Kuo et al., 2012). These measurements, displayed in Figure 1 (a), are primarily located at Taiwan Strong Motion Instrumentation Program (TSMIP) stations and the velocities were measured with the P-S suspension logging technique developed by OYO Corporation; the drilling did not reach 30 m at 54 of these sites and so the profile had to be extrapolated to compute V_{S30} as described by Kuo et al. (2011).

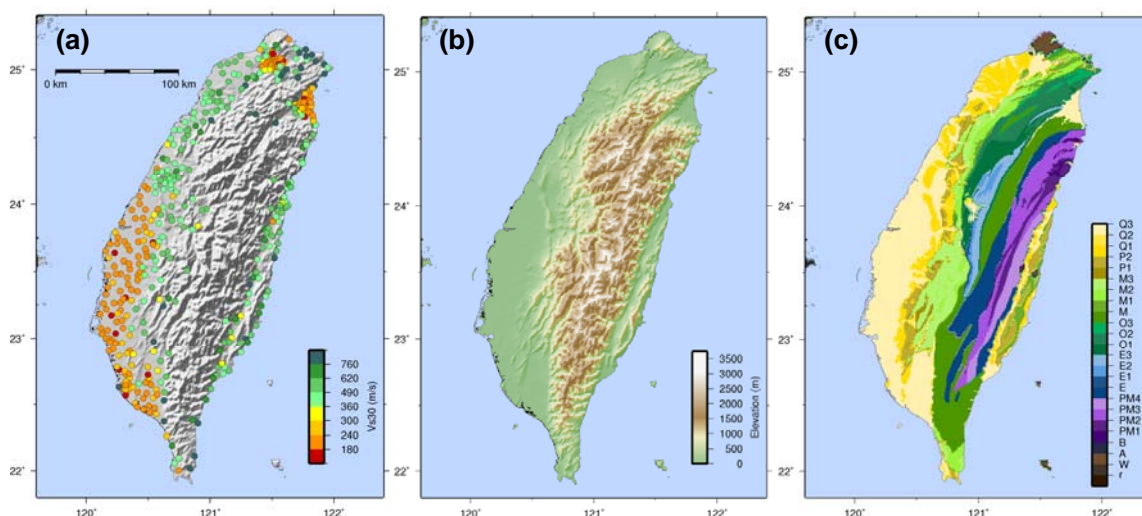


Figure 1. (a) NCREE V_{S30} measurements (Kuo et al., 2012). (b) SRTM 30c topography. (c) Geologic units compiled by Lee et al. (2001).

3. CHOICE OF TOPOGRAPHIC RESOLUTION

The relationship between V_{S30} and topographic gradient was originally based on SRTM 30c data (Wald and Allen, 2007). These data have a pixel size of approximately 900 m. Allen and Wald (2009) investigated the use of high resolution topography. They found that the higher resolution data is better at defining spatial features, such as the shape of a sedimentary basin, but that the correlation with V_{S30} is not any stronger than when the 30c data is used. We revisit this issue here by plotting the NCREE V_{S30} data against the gradient at two resolutions in Figure 2. Figure 2 (a) uses the gradient from 30c SRTM data, while Figure 2 (b) uses the gradient calculated from 9c SRTM data (about 270 m pixel size). The Allen and Wald (2009) relationship is plotted as a line on each plot. The key difference is the behaviour at slopes less than $3e-3$. There are far fewer sites with slopes in this range at the 9c resolution, while the sites with slopes in this range at the 30c resolution all tend to have relatively low

V_{S30} values. These slower velocity sites are thus mixed with faster sites when plotted against 9c gradients. In this way, better spatial resolution (i.e., pixel size) does not result in a better estimate of V_{S30} . For these reasons, our subsequent analysis makes use of the 30c data for Taiwan.

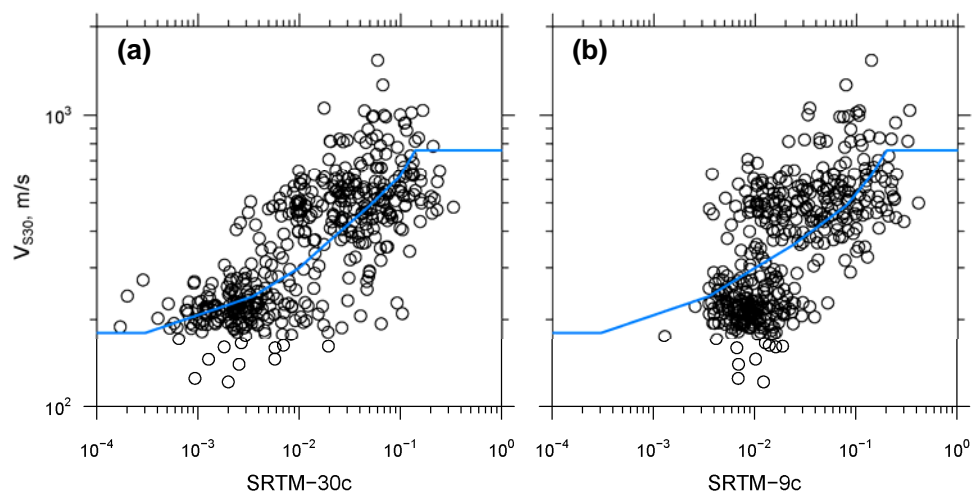


Figure 2. V_{S30} measurements (Kuo et al., 2012) plotted against gradients computed from (a) SRTM 30c topography, and (b) SRTM 9c topography.

4. GROUPING SIMILAR GEOLOGIC UNITS

Geology is a valuable predictor of V_{S30} (e.g., Wills and Clahan, 2006) but if we are to use the mapped geologic units in Figure 1 (c) to assign V_{S30} values then each geologic unit must contain adequate V_{S30} measurements to constrain the average value. Unfortunately, only 15 of the 24 Lee et al. (2001) geologic units contain at least one V_{S30} measurement and only nine units have five or more measurements. Thus, we need to aggregate the geologic units into simpler geologic groupings. This is an important choice, one that must be exercised anywhere existing geologic maps are used for this purpose. For site response purposes, we are particularly interested in distinguishing between the velocities of younger sediments. This priority is reflected by the density of the V_{S30} measurements in Figure 1 (a), which are clustered in the relatively flat regions that also corresponds to the younger units of Figure 1 (c). With this in mind, we group these units into four categories shown in Figure 3 and summarized in Table 1. Note that the Holocene unit corresponds directly to Q3, and the Pleistocene unit is composed of Q1 and Q2. Ideally, we would separate the Holocene unit into more subdivisions based on grain size, sediment depth, or other important characteristics. But we do not have this type of information at the scale of this map.

Table 1. Summary of the simplified geologic classifications.

Symbol	Description	Number of Measurements	Geometric mean V_{S30} (m/s)	Standard deviation (base 10 log units)
H	Holocene	297	297	0.198
P	Pleistocene	73	479	0.116
T	Tertiary Rock	68	576	0.170
R	Other Rock	9	491	0.153

5. HYBRID VS30 MAPPING STRATEGY

We consider two different approaches to combining the slope and geology information into a single map of V_{S30} . The two different strategies reflect different interpretations of the relationships between V_{S30} , gradient, and geology. The two strategies described below are different ways of defining the

“trend” of V_{S30} for a region. An additional step that we add to both of these strategies is the “kriging-with-a-trend” geostatistical method (Cressie, 1993). This method, as other geostatistical methods, is effective because it takes advantage of the spatial correlation structure of the residuals and can substantially improve the accuracy of site response maps, effectively making the maps consistent with the available measurements (Thompson et al., 2010). The primary advantage of this method over ordinary kriging is in the performance at locations far from the measurements approach the “trend” in the model, which is defined by slope and surface geology in this paper. In this way, the kriging-with-a-trend method is a flexible model that uses the measurements to predict V_{S30} where they are available but also takes advantage of geologic and topographic information in locations that are not near measured values.

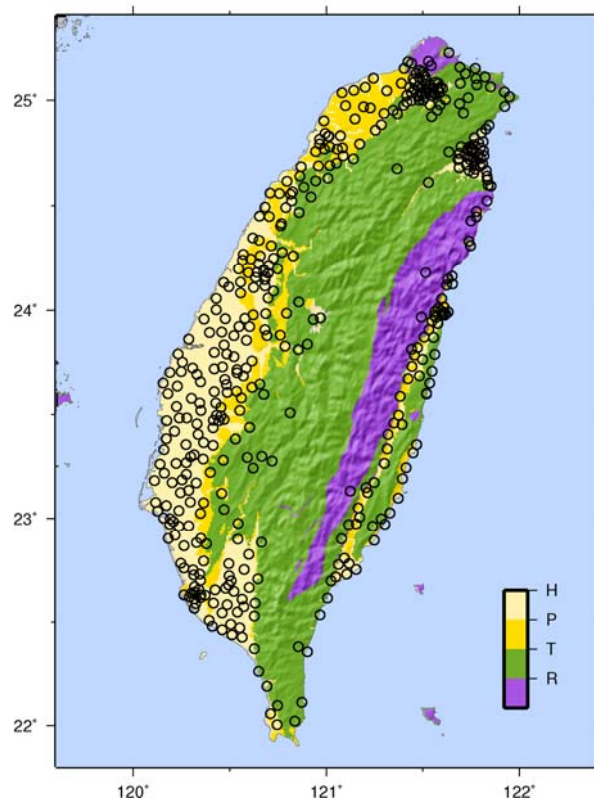


Figure 3. Map of the simplified geologic units summarized in Table 1. The open circles indicate the location of V_{S30} measurements.

5.1. Hybrid Strategy 1

Since the slope-based V_{S30} estimates are available globally, it is convenient to use this as a baseline model. Thus, our first approach is to use the simplified geologic classes to locally refine the map. This is an approach that could be followed in any region with significant number of V_{S30} measurements and surface geology map to improve upon the slope-only model. The algorithm for combining slope and geology is very simple: (1) compute the slope-based V_{S30} for the region, (2) compute the residual at each measured V_{S30} value, (3) compute the mean residual for each geologic grouping, and (4) use the mean residual to update the map based on the geologic unit. We assume that V_{S30} is lognormally distributed (this is why we use the geometric mean in Table 1). When working with a lognormally distributed variable, it is convenient to work with the logarithmic residuals. However, we prefer to use the residual ratio (measured V_{S30} /predicted V_{S30}) because it is an easier number to interpret. Figure 4 illustrates this first strategy by plotting: (a) the map of V_{S30} predicted by the Allen and Wald (2009) model, (b) the mean residual ratio for each of the simplified geologic classes, and (c) the result when the Allen and Wald (2009) model is multiplied by the mean residual ratio of each geologic unit.

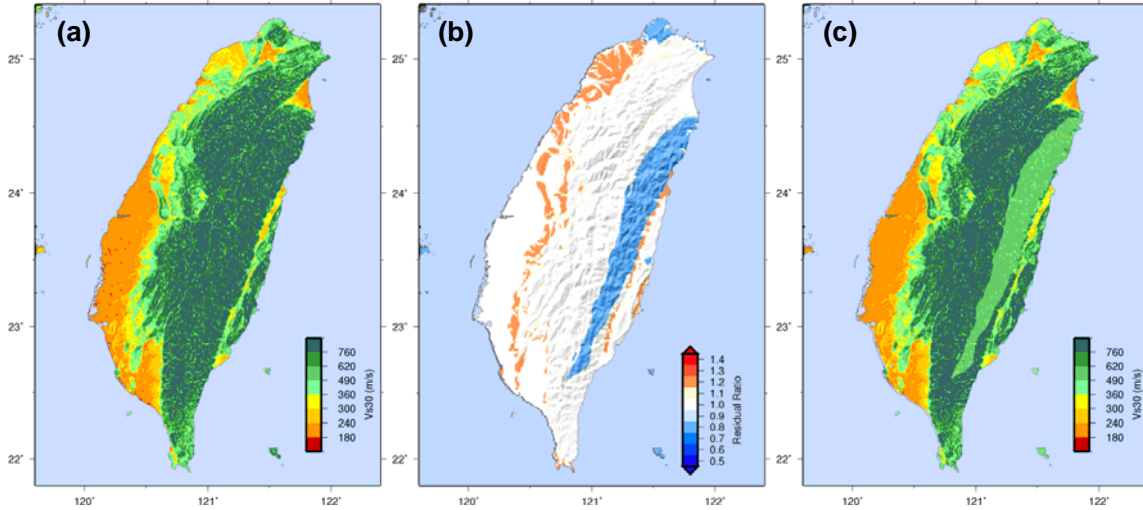


Figure 4. (a) V_{S30} computed with the Allen and Wald (2009) method, (b) Mean residual ratio in each the simplified geologic categories, and (c) the V_{S30} map that results from multiplying (a) and (b).

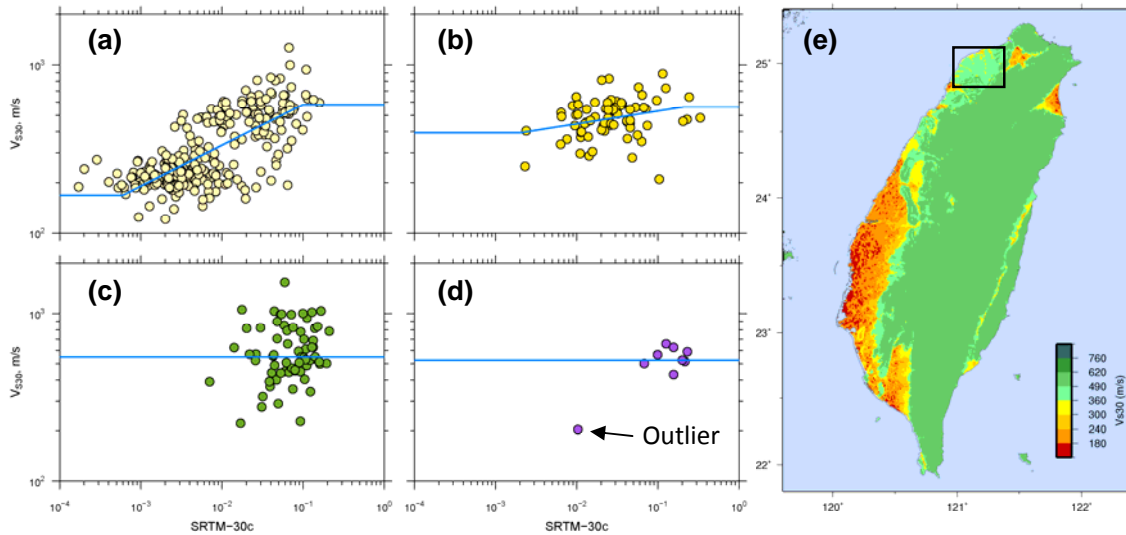


Figure 5. V_{S30} vs slope for (a) Holocene, (b) Pleistocene, (c) Tertiary rocks, and (d) other rock units; (e) is the map that results from applying these relationships. The outlier discussed in the text is labeled with an arrow in (d). The example region discussed in the text that is primarily Pleistocene units in (e) is labeled with a box.

5.2. Hybrid Strategy 2

An alternative method to combine slope and geology is to assume that there may exist a different relationship between slope and V_{S30} for each geologic unit. To investigate this possibility, we plot V_{S30} as a function of slope for each geologic unit in Figure 5. Figure 5 shows that the strongest relationship between slope and velocity is in the Holocene units, while the Pleistocene units show only a relatively weak trend. Note, however, that both the V_{S30} values and the slopes tend to be larger in the Pleistocene relative to the Holocene, as we would expect. The V_{S30} measurements Tertiary rock exhibit a large amount of variability but do not exhibit a trend with slope. It is interesting to note how the slope

values within the Tertiary units are all relatively large when compared to the younger units. But at the same time there is a large range in V_{S30} values. We interpret this as an indication that although slope and geology are in agreement that these sites are located in rock (classified as Tertiary rock and have large slopes) there is still a large range in the V_{S30} measurements from 222 m/s to 1538 m/s. This highlights the limitations of applying either of these proxy methods in mountainous regions. There are only 9 measurements in the ‘other rock’ category (R) and so it is difficult to draw conclusions. We would like to note, however, that the outlier at low slope and low V_{S30} is very close to the geologic contact between Holocene and the ‘other rock’ category, and so this outlier may be attributed to a misclassification due to the limited precision of the geologic map and the station waypoints. The blue lines in Figures 5 (a) and (b) are determined with a piecewise-linear regression. The lack of trend in Figures 5 (c) and (d) led us to use the median V_{S30} for these units, which is represented by the horizontal blue line. Figure 5 (e) is the map that results when the slope- V_{S30} relationship represented by the blue lines in Figures 5 (a) through (d) is applied to the SRTM 30 c data.

The limited range of the mapped values with the second hybrid strategy is problematic because there are no site classes A or B ($V_{S30} > 760$ m/s). Comparing Figure 5 (e) with Figures 4 (a) and 4 (c) illustrates that the median measured V_{S30} values for the rock sites is surprisingly small. The faster velocities in Figure 4 (a) and (c) come from the slope- V_{S30} relationship, which is largely inferred because of the lack of site class V_{S30} measurements in site classes A and B. The reason for the lack of observations in hard rock sites likely arises from choices made in selecting strong motion stations, resulting in a sampling bias in terms of both V_{S30} and gradient. We also observe that the second mapping strategy results in significantly more site class E in the coastal regions. The piecewise-regression by geologic unit strategy, however, does not result in uniformly smaller values than the first approach of refining the Allen and Wald (2009) method with the geologic units. For example, there is a region west of Taipei that is primarily mapped as Pleistocene units (approximately 121°E, 25°N) that is uniformly faster in Figure 5 (e).

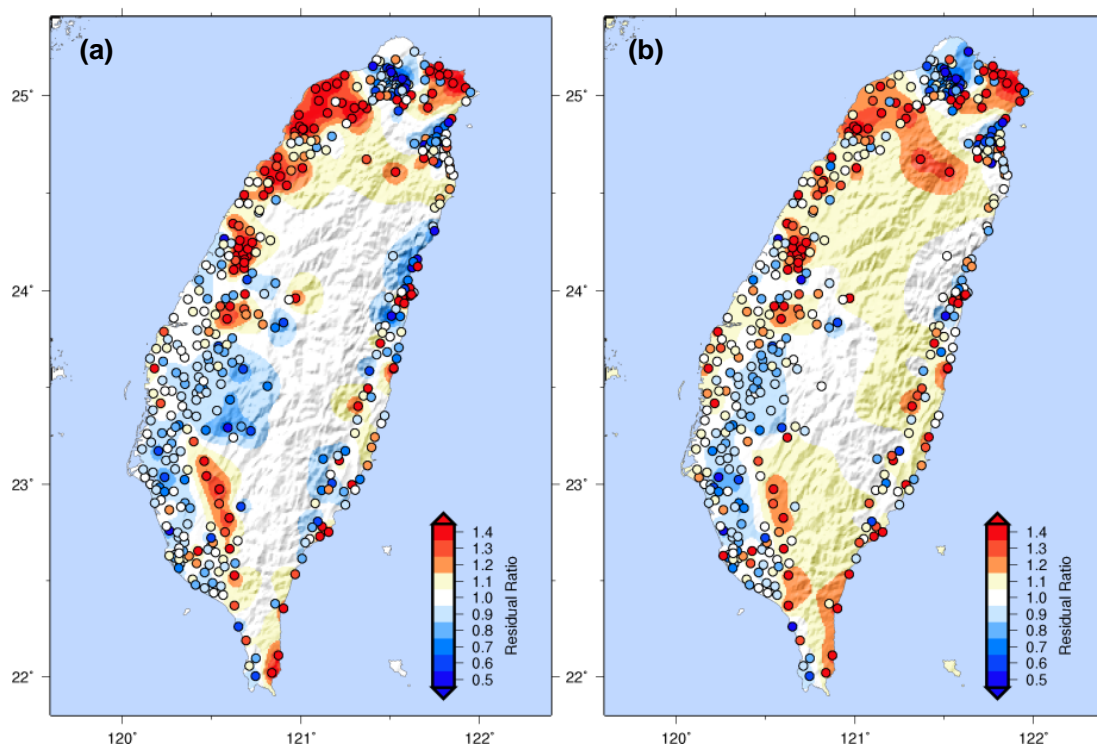


Figure 6. Residuals at the V_{S30} measurements and the kriged values for (a) Strategy 1 – refining the Allen and Wald (2009) approach with the Lee et al. (2001) surface geology (see Figure 4c), and (b) Strategy 2 – a separate piecewise-regression of the slope- V_{S30} relationship for each geologic classification (see Figure 5).

5.3. Final V_{S30} Maps

The prior maps all represent methods for defining the trend of V_{S30} as a function slope and geology. However, we are unable to capture certain spatial trends with these variables. Thus, we use the kriging-with-a-trend strategy which brings the maps into much closer agreement with the dense coverage of V_{S30} measurements. The spatial structure of the residuals is illustrated in Figure 6. These maps indicate that there are still regions where the V_{S30} is consistently over-estimated or under-estimated. For example, there is a region at about 23.5°N and 120.5°W where most of the residuals are less than unity, indicating that the map is over-predicting the measurements. This trend is more prominent in Figure 6 (a) than (b). Figure 7 gives the maps that correct for the remaining spatial correlation structure illustrated in Figure 6. In areas with dense coverage of V_{S30} measurements, the two maps give similar results as we should expect. The major differences are in the mountainous regions, which reflect the uncertainty of the velocities in these regions. As noted by Wald and Allen (2007), this uncertainty may not be very important from a risk perspective because V_{S30} -based amplification factors are uniformly small over a wide range of rock V_{S30} values and the population is largely located in the slower flatlying coastal regions where the V_{S30} is much better constrained. There are other uses of V_{S30} maps, such as identifying reference rock sites for developing ground motion equations, where constraining the V_{S30} in rock is a critical issue.

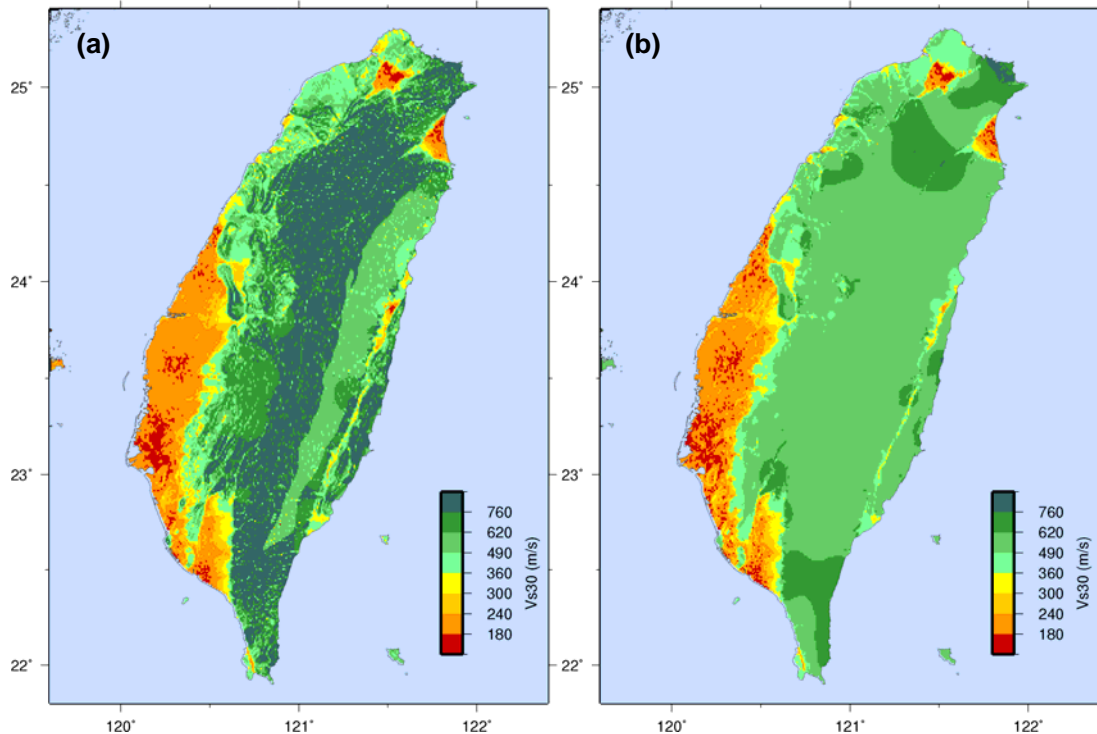


Figure 7. Final V_{S30} maps using the kriging-with-a-trend method where the trend is defined as a function of gradient and surface geology for (a) Strategy 1, and (b) Strategy 2.

6. MODEL UNCERTAINTY

We compare the accuracy of the different maps in terms of the standard deviation of the logarithmic residuals (σ). We include a geology-only model that predicts the mean values reported in Table 1, a slope-only model that uses the Allen and Wald (2009) predicts, the hybrid strategy 1 illustrated in Figure 4 (c), the hybrid strategy 2 illustrated in Figure 5 (e), and the two kriging-with-a-trend models that define the trend as the two alternative hybrid models. For the kriging models, we use the leave-

one-out cross validation strategy to compute the residuals at a given location. The values of σ for these different mapping strategies are reported in Figure 8. We see that the geology-only approach as the largest uncertainty. We acknowledge, however, that this is only one relatively coarse geology-based model. The use of finer scale surface geology maps and further separation of the Holocene unit would lead to significant improvement in the accuracy of this approach. At this national scale, however, the σ for the Allen and Wald (2009) (AW09) slope-only model is about 19% smaller than the geology-only approach. Refining the AW09 model with the mean geology residuals (hybrid strategy 1) results in a σ that is about 2% smaller than that for AW09. The second hybrid strategy that uses a separate slope- V_{S30} relationship for the four different geologic categories (labelled “AW09+PRG”) gives results in a sigma that is about 6% smaller than that for AW09. When the residuals are then kriged for these two hybrid methods, σ is reduced by 12% and 16%, respectively, relative to the AW09 model. It is important to bear in mind that the values reported in Figure 8 reflect the sampling bias in the V_{S30} dataset; the larger uncertainty of the V_{S30} map in the mountainous regions are undersampled.

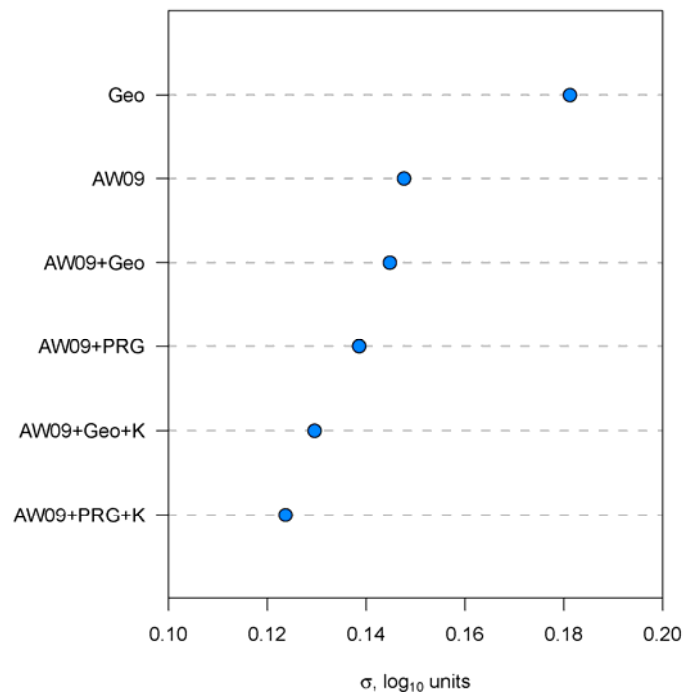


Figure 8. Summary of σ (standard deviation of the logarithmic residuals) for the different V_{S30} mapping strategies that we have applied to Taiwan. The shortened labels are defined as follows: Geo refers to the simplified geology model; AW09 refers to the Allen and Wald (2009) slope-based model; AW09+Geo refers to the AW09 model corrected for the mean residual in each of the simplified geologic units (Figure 4); AW09+PRG refers to the piecewise regression by geologic unit (Figure 5); AW09+Geo+K is the AW09+Geo model along with kriged residuals; AW09+PRG+K is the AW09+PRG model with kriged residuals.

7. SUMMARY

The topographic slope method of estimating site response is often the only available estimate of V_{S30} for regional mapping purposes. Some regions have additional geospatial information that can be used to constrain V_{S30} estimates. This includes maps of surface geology, but microzonation maps based on dense coverage of in situ measurements are also available for some urban areas with large populations exposed to heightened seismic hazard. We use Taiwan as an example to study alternative approaches to combine these available data to produce a V_{S30} map. We use the kriging-with-a-trend geostatistical method, where the different geology-slope hybrid models define the “trend” in this procedure. One benefit of this geostatistical approach is that it identifies spatial patterns in the map that are not

detected by the combination of slope and geology. Additionally, unlike current state-of-the-art V_{S30} mapping strategies, this approach locally refines the map in the vicinity of the measurements where V_{S30} is known with greater confidence than the estimate based on correlations with geology and/or slope. The extensive database of V_{S30} measurements allows us to quantify the improvement in accuracy that we can achieve when we include these additional constraints on the V_{S30} map. For Taiwan, we are able to achieve a reduction in the uncertainty of about 16% relative to the globally applicable topographic slope method.

ACKNOWLEDGEMENT

We thank Harold Magistrale and Bill Stephenson for providing thoughtful reviews.

REFERENCES

- Abrahamson, N., Atkinson, G., Boore, D.M., Bozorgnia, Y., Campbell, K., Chiou, B., Idriss, I.M., Silva, W., and Youngs, R. (2008). Comparisons of the NGA ground-motion relations. *Earthquake Spectra* **24**, 45-66.
- Allen, T.I., and Wald, D.J. (2009). On the Use of High-Resolution Topographic Data as a Proxy for Seismic Site Conditions (V_{S30}). *Bull. Seism. Soc. Am.* **99**, 935-943.
- Cressie, N.A.C. (1993). *Statistics for Spatial Data*. John Wiley & Sons, Inc., New York.
- Holzer, T.L., Padovani, A.C., Bennett, M.J., Noce, T.E., and Tinsley, J.C. III (2005). Mapping NEHRP VS30 site classes. *Earthquake Spectra* **21**, 353-370.
- International Code Council (2006). International Building Code, Falls Church, Virginia.
- Kuo, C.H., Wen, K.L., Hsieh, H.H., Chang, T.M., Lin, C.M., and Chen, C.T. (2011). Evaluating empirical regression equations for V_s and estimating V_{S30} in northeastern Taiwan. *Soil Dynamics and Earthquake Engineering* **31**, 431-439.
- Kuo, C.-H., Wen, K.-L., Hsieh, H.-H., Lin, C.-M., Chang, T.-M., and Kuo, K.-W. (2012). Site classification and V_{S30} estimation of free-field TSMIP stations using the logging data of EGDT. *Engineering Geology* **129-130**, 68-75.
- Lee, C.-T., Cheng, C.-T., Liao, C.-W., and Tsai, Y.-B. (2001). Site classification of Taiwan free-field strong-motion stations. *Bull. Seism. Soc. Am.* **91**, 1283-1297.
- Magistrale, H., Rong, Y., Silva, M., and Thompson, E.M. (2012). A Site Response Map of the Continental U.S., 15th World Conference on Earthquake Engineering, Lisbon, Portugal.
- Petersen, M.D., Frankel, A.D., Harmsen, S.C., Mueller, C.S., Haller, K.M., Wheeler, R.L., Wesson, R.L., Zeng, Y., Boyd, O.S., Perkins, D.M., Luco, N., Field, E.H., Wills, C.J., and Rukstales, K.S. (2008). Documentation for the 2008 Update of the United States National Seismic Hazard Maps: U.S. Geological Survey Open-File Report 2008-1128, 61 p.
- Romero, S., and Rix, G.J. (2001). Regional Variations in Near-Surface Shear Wave Velocity in the Greater Memphis Area. *Engineering Geology* **62**, 137-158.
- Thompson, E. M., Baise, L.G., Kayen, R.E., Morgan, E.C., and Kaklamanos, J. (2011). Multiscale site-response mapping: a case study of Parkfield, California. *Bull. Seism. Soc. Am.* **101**, 1081-1100.
- Thompson, E.M., Baise, L.G., Kayen, R.E., Tanaka, Y., and Tanaka, H. (2010). A Geostatistical Approach to Mapping Site Response Spectral Amplifications. *Engineering Geology*. **114**, 330-342.
- Tinsley, J.C., and Fumal, T.E. (1985). In: Ziony, J.I. (Ed.), Mapping quaternary sedimentary deposits for areal variations in shaking response: Evaluating Earthquake Hazards in the Los Angeles Region-An Earth Science Perspective, 101-125.
- Wald, D.J., Allen, T.I., (2007). Topographic Slope as a Proxy for Seismic Site Conditions and Amplification, *Bull. Seism. Soc. Am.* **97** (5), 1379-1395.
- Wald, D.J., McWhirter, L., Thompson, E.M., and Hering, A.S. (2011). A New Strategy For Developing V_{S30} Maps, *4th IASPEI/IAEE International Symposium: Effects of Surface Geology on Seismic Motion*. August 23-26, Santa Barbara, USA.
- Wills, C.J. and Clahan, K.B. (2006). Developing a Map of Geologically Defined Site-Condition Categories for California. *Bull. Seism. Soc. Am.* **96**, 1483-1501.
- Yong, A., Hough, S.E., Abrams, M.J., Cox, H.M., Wills, C.J., and Simila, G.W. (2008). Site Characterization Using Integrated Imaging Analysis Methods on Satellite Data of the Islamabad, Pakistan, Region. *Bull. Seism. Soc. Am.* **98**, 2679-2693.
- Yong, A., Hough, S.E., Iwahashi, J., and Braverman, A. (2012). A Terrain-Based Site-Conditions Map of California with Implications for the Contiguous United States. *Bull. Seism. Soc. Am.* **102**, 114-128.